

SIMULATION OF ULTRASONIC EXAMINATIONS USING SURFACE ACOUSTIC WAVES

N. Leymarie¹, A. Lhémy¹, P. Calmon¹, S. Chatillon¹ and R. Coulette²

¹ Commissariat à l'Énergie Atomique, CEA-Saclay, Gif-sur-Yvette cedex, France

² SNECMA Moteurs, Évry cedex, France

Abstract: The UT simulation tools developed at the French Atomic Energy Commission (CEA) in the CIVA software platform were up to now limited to methods based on bulk ultrasonic waves. This study aims at extending the capabilities of the models to deal with testing configurations using surface acoustic waves (SAW). In such configurations, specific transducer arrangement is made to generate and receive surface waves. Very often, the field is generated by refracting a bulk longitudinal beam at the surface under test at a specific angle (e.g. Rayleigh angle).

In the present work, a model has been derived to predict the SAW wavefield in the part under test by an arbitrary transducer as well as the leaky surface acoustic wave associated to the SAW propagation radiated in the coupling medium. First, asymptotic expressions for SAW and leaky surface waves are derived in the case of a point source radiating from a fluid medium over an elastic half-space. A geometrical interpretation is proposed allowing to derive a more general model based on the pencil method. Fields radiated by an arbitrary transducer are obtained and expressed as impulse responses to be convolved with an excitation pulse to quantitatively predict useful quantities (particle displacement, stress etc...). Examples of surface wavefields computed by the proposed model are given and compared with exact results (planar interface) showing its accuracy. The method should allow one to predict surface wavefields not only at planar surfaces but also propagating along curved surfaces described by CAD or analytically.

Introduction: NDT simulation plays an increasingly important role at various stages in the design-processing-manufacturing-service chain of events [1]. It makes easier the design of new NDT methods, helps to demonstrate the performances of already existing or newly developed ones (performance demonstration, qualification), to interpret experiments (through simple comparison of measured data with predicted ones or more sophisticated model-based inversion algorithms). This is principally true for quantitative NDT methods such as ultrasonic testing (UT).

For more than a decade, the French Atomic Energy Commission has been developing a platform software called CIVA that includes various quantitative UT simulation tools, together with tools for eddy-current methods [2]. Currently, CIVA simulation tools can handle very complex UT configurations: parts may be of complex geometry defined by 3D-CAD and composed of heterogeneous and anisotropic materials. Arbitrary transducers can be also considered (used in immersion or contact configuration, monolithic or phased-arrays), used in pulse-echo or in pitch-catch configurations. Similarly, various geometries of defects within the elastic medium can be accounted for and different scattering theories are used depending on defect geometry and position in the part. Only semi-analytic modeling can permit to handle such a complexity while keeping computation time compatible with intensive use of the software.

Until now and as far as UT is concerned, most of the efforts in developing modeling tools and associated software were dedicated to methods relying on bulk wave propagation into parts. The present paper is dedicated to the development of new capabilities to deal with UT methods involving surface wave propagation.

Previous to the development presented hereafter, our experience in modeling testing configurations involving surface waves was based on two developments which are briefly described. The first modeling work was carried out for the development of an original method of characterization of elastic properties of materials using Rayleigh wavespeed measurement similar to what is done in acoustic microscopy, that is, based on inversion of the so-called $V(z, \theta)$ curves. The originality in this work is that these curves are measured using a specific phased-array transducer that avoids transducer motion relatively to the part under test but rather uses computerized delay-laws to simulate z translation and θ rotation [3]. A model has been developed to, first, properly optimize the transducer design and further to simulate the effects of the various parameters of this configuration on measurement accuracy. The method being based on leaky Rayleigh wave measurements, the model deals with the decomposition of the incident field radiated at the interface between the water coupling and the part into a spectrum of plane waves which makes reflection easy to compute. Once the various reflection coefficients are computed, an inverse

transform of the reflected plane waves allows the prediction of both specular and non-specular reflection phenomena, these including leaky Rayleigh wave generation.

The second modeling work involving Rayleigh waves was carried out when considering the generation of Rayleigh waves by diffraction of an incident bulk wave at a crack edge, their propagation onto the crack surface and their scattering by crack edges as both bulk and surface waves. In this study, the various phenomena are modeled by means of a theoretical transient formulation of the Geometrical Theory of Diffraction for elastic waves, that is, an approximate formulation based on high frequency asymptotics. In this theory, the various phenomena can be interpreted geometrically [4].

The solution presented here to simulate UT using surface waves benefits from these two previous experiences. From the former, exact results can be obtained and used as reference results very helpful to check the accuracy of an approximate solution. From the latter, the possibility of developing asymptotic solutions is demonstrated, this allowing easy-to-understand geometrical interpretation of surface wave propagation and scattering.

Of primary interest is the development of a tool for predicting the wavefield radiated by a transducer. A detailed description of how the energy is radiated depending on transducer diffraction effects is a very useful information in itself and in practice, the choice of a transducer is greatly helped by such a result. Moreover, this constitutes an input for the simulation of an experiment involving the interaction of an incident wavefield with a defect. Such a tool may be therefore seen as the kernel of any model involving surface wave propagation.

The tool is expected to deal with parts not necessarily planar and with arbitrary transducers to be included in CIVA that deals with these cases when bulk waves are concerned. Moreover, our experience in the development of the model and software for predicting fields of bulk waves leads us to seek a solution for the surface waves compatible with the existing solution for the bulk waves, based on the pencil method [5].

To deal with arbitrary ultrasonic sources, the source surface is discretized as a set of source points of infinitesimal surface. Predicting transducer diffraction effects at a given field point requires the solution for the field radiated at this field point by a source point to be integrated over the discrete surface of the transducer. These effects are predicted in exactly the same way for bulk waves. What differs from one case to the other is the elementary solution used. However, surface waves are generally generated by refracting an incident beam of bulk waves at the critical angle corresponding to the surface wave speed. The radiation of the beam of bulk waves involved in the surface wave generation may simply be computed using the existing code. The way of accounting for non-planar interfaces is presented in the paragraph dedicated to discussions.

The contributions of a source point P in the fluid (see Figs. 1 and 2) at a field point in the fluid after scattering by the planar interface with the solid can be written as exact integral formulations [6,7]. For the reflected waves in the fluid, the Fourier transform of the scalar potential response $\bar{\varphi}_{refl}(M/P)$ at a point M from writes:

$$\bar{\varphi}_{refl}(M/P) = \bar{\varphi}_0 j k_0 \int_{\Gamma} R(\theta) H_0^{(1)}(k_0 r \sin \theta) e^{jk_0 |z_M + z_P| \cos \theta} \sin \theta d\theta \quad (1)$$

where $\bar{\varphi}_0$ is the scalar potential of the source, k_0 the wavenumber in the fluid, $R(\theta)$ the reflection coefficient at the interface for an incident θ angle and Γ is the complex integral path from $j\infty - \pi/2$ to $\pi/2 - j\infty$. A semi-analytical approximation of this integral can be performed by the saddle point method [8]. The asymptotic solution allows the independent evaluation of the various specular (reflected wave) and non-specular (the longitudinal and transverse head waves and the Rayleigh wave) contributions. The Rayleigh wave contribution is derived as a pole integral contribution. In the fluid, the (leaky) Rayleigh wave contribution writes:

$$\bar{\varphi}_{Rayleigh_fluid}(M/P) \approx \bar{\varphi}_0 \frac{A_{fluid}(\omega)}{\sqrt{r}} e^{-\alpha_R L_R} e^{j\omega \left(\frac{L_P + L_M}{c_0} + \frac{L_R}{c_R} \right)}, \quad (2)$$

where A_{fluid} is a complex amplitude coefficient, c_0 is the wavespeed in the fluid and c_R that of the Rayleigh wave. α_R accounts for the attenuation coefficient of the Rayleigh wave and L_P, L_M, L_R and r denote distances as shown in Fig. 1. Let us define θ_R , the Rayleigh angle, by:

$$\theta_R = \arcsin(c_0 / c_R). \quad (3)$$

A ray interpretation of Eq. (2) can be given describing the various ray paths and associated time-of-flights $(L_P+L_M)/c_0+L_R/c_R$ or attenuation due to leakage ($e^{-\alpha_R L_R}$). Figure 1 depicts this interpretation.

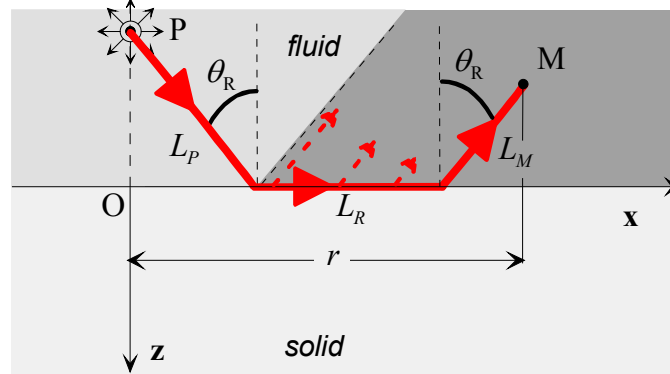


Figure 1: Geometrical path of the Rayleigh wave contribution in the fluid from the source point P to the observation point M . Dashed arrows along L_R denote the leakage of the Rayleigh wave into the fluid.

We derived the Rayleigh wave contribution in the solid by following the same procedure as in [8]. The integral expressions of the scalar and vector potentials are also evaluated asymptotically. By introducing the expression for the potential $\bar{\varphi}_{Rayleigh_fluid}(M'/P)$, where M' is the closest point of the interface to M , these solutions write:

$$\begin{cases} \bar{\varphi}_{Rayleigh_solid}(M/P) \approx \bar{\varphi}_{Rayleigh_fluid}(M'/P) \times A_L(\omega) \times e^{-\alpha_L MM'} \\ \bar{\psi}_{Rayleigh_solid}(M/P) \approx \bar{\varphi}_{Rayleigh_fluid}(M'/P) \times A_T(\omega) \times e^{-\alpha_T MM'} \end{cases} \quad (4)$$

where A_L (resp. A_T) is a complex-valued conversion coefficient of the potential in the fluid into scalar potential (resp. vector potential) in the solid. α_L and α_T are two coefficients for the attenuation away from the interface of the longitudinal and transverse waves, respectively. Thus, the ray interpretation of Eq. (4) is the same as that for the contribution in the fluid from the source P to M' . From point M' to M , the longitudinal (resp. transverse) component of the Rayleigh wave is simply attenuated by a factor of $e^{-\alpha_L MM'}$ (resp. $e^{-\alpha_T MM'}$) (see Fig 2).

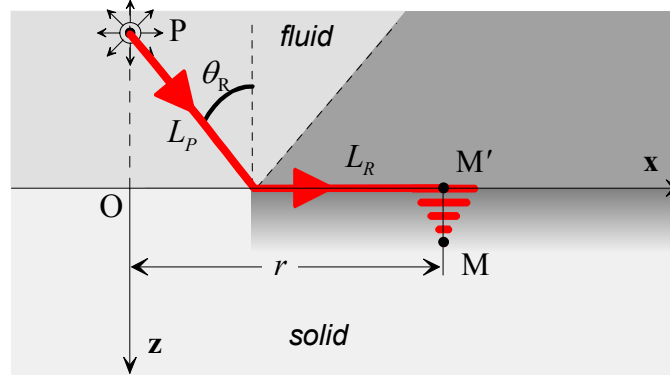


Figure 2: Geometrical path of the Rayleigh wave contribution in the solid from the point source P to the observation point M .

In the previous expressions, independently of the attenuation terms describing the leakage, the amplitude decreases as $r^{-1/2}$. This is typical of the divergence of a wave in a 2D space and nothing but the divergence factor of the Rayleigh wave for the propagation shown in Fig. 3. r accounts for the path on the interface and the projection on the interface of the bulk wave paths in the fluid.

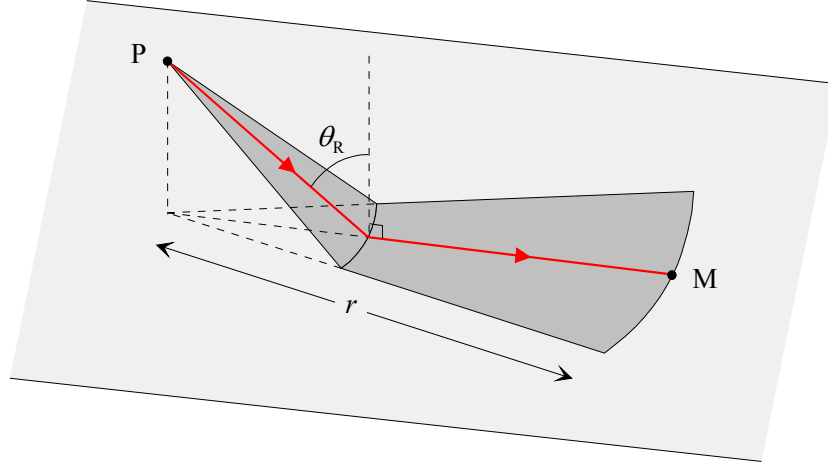


Figure 3: Two-dimensional divergence of the Rayleigh wave pencil.

Results: In this section, the model derived from the previous asymptotic expressions is validated by comparing its predictions with exact integral calculations for a point source in the fluid. All the results are obtained in the case of a planar part made of Titanium immersed in water. Material properties from which Rayleigh wave characteristics are deduced are given in Table 1.

Material properties			Rayleigh wave	
water	ρ_0 (g/cm ³)	1.0	θ_R	28.88°
	c_0 (mm/ μ s)	1.482	c_R (mm/ μ s)	3.068
titanium	ρ (g/cm ³)	4.5	α_R (dB/mm/MHz)	0.32
	c_L (mm/ μ s)	6.070	α_L (dB/mm/MHz)	15.38
	c_T (mm/ μ s)	3.310	α_T (dB/mm/MHz)	6.74

Table 1: Properties of the water/titanium interface used in the calculations and the deduced characteristics of the Rayleigh wave.

Figure 4 compares the exact response (from Eq. 1) with the Rayleigh wave contribution predicted by the present model. The source point P is located at the height 200 mm above the plane generating a pulse of 2 MHz center frequency and the observation point M is at the same height and at a distance of 200 mm chosen so that the reflected angle of the specular wave is greater than θ_R . It can be seen from the figure that the exact integral calculation predicts different contributions generated at the interface, whereas the asymptotic model was used to only evaluate the Rayleigh contribution. For this wave, an excellent agreement is obtained.

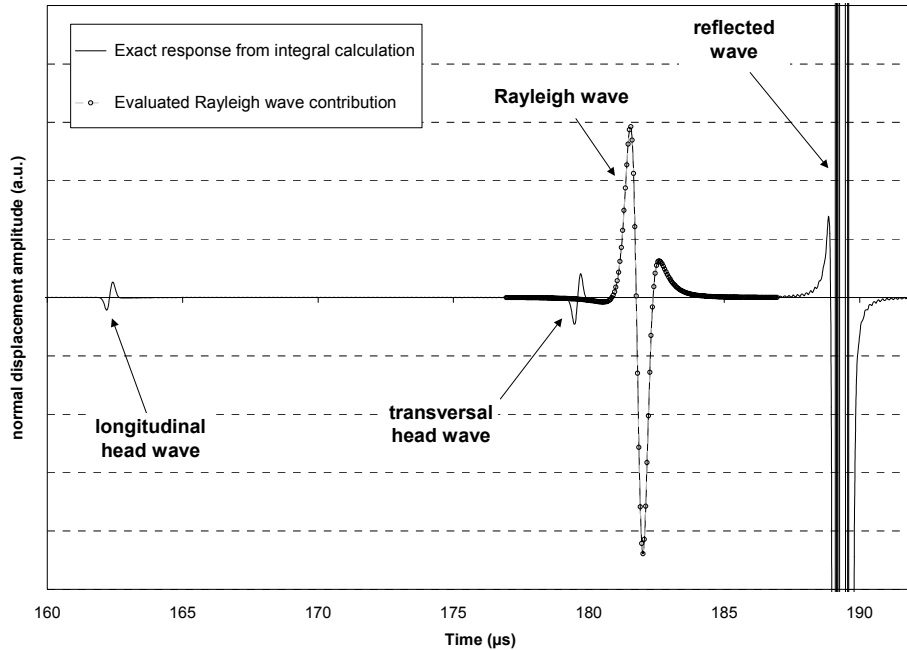


Figure 4: Comparison of the exact response with the asymptotic Rayleigh wave contribution at a field point in the coupling fluid.

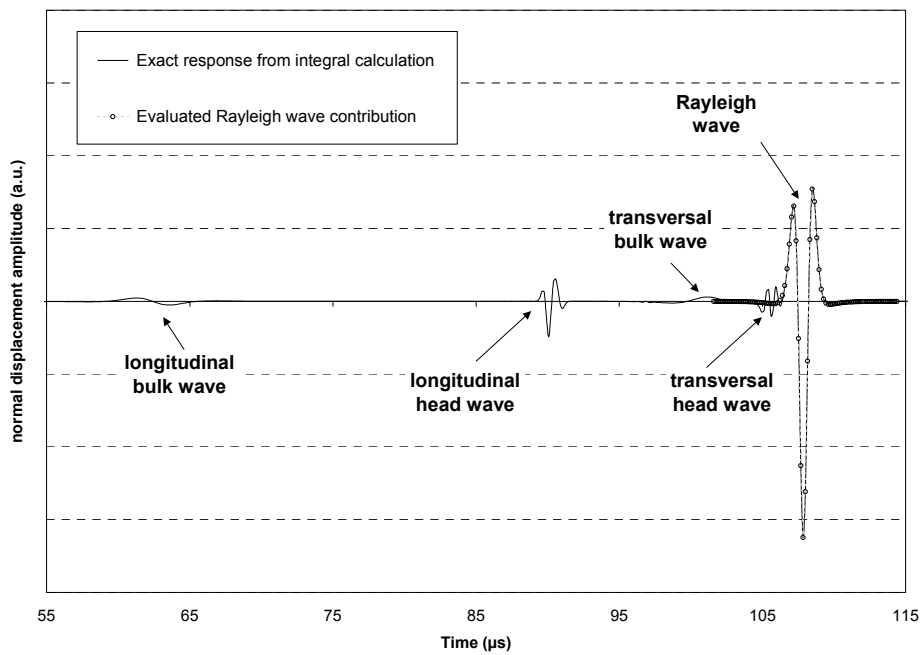


Figure 5: Comparison of the exact response with the asymptotic Rayleigh wave contribution at a field point in the solid.

A similar comparison is given on Fig. 5 for an observation point in the solid at a depth of 2 mm and at a distance of 150 mm along the plane. The Rayleigh wave being highly attenuated within the thickness, the effective depth of penetration is only a few wavelengths. Again, extremely good agreement is found between the exact integral calculation and the asymptotic method for the Rayleigh wave.

Now that the asymptotic expression for the Rayleigh wave has been validated, it may be used for the prediction of transducer diffraction effects. The comparison with corresponding exact results is now out of reach since the evaluation of the whole integral solution is very computer intensive, considering the number of source points to

take into account. Only the asymptotic solution offers high performances. Figure 6 shows the displacement field normal to the interface (z direction) for a transducer oriented at the Rayleigh angle θ_R in order to generate mainly the Rayleigh wave. In this figure, only the Rayleigh wave contribution is shown. Calculations have been performed in CIVA for a 20 mm diameter flat transducer with a center frequency of 2 MHz.

Both the Rayleigh wave in the solid and its leakage in the fluid are displayed. The display window is that of CIVA originally developed for bulk waves. In these results, Rayleigh and leaky Rayleigh waves were computed (then, displayed) independently of bulk wave contributions. The field amplitude of the surface wave decreases with its propagation along the interface due to the leakage phenomenon. Note that the Rayleigh wave propagating in the solid and its leakage in the coupling fluid are continuous across the interface.

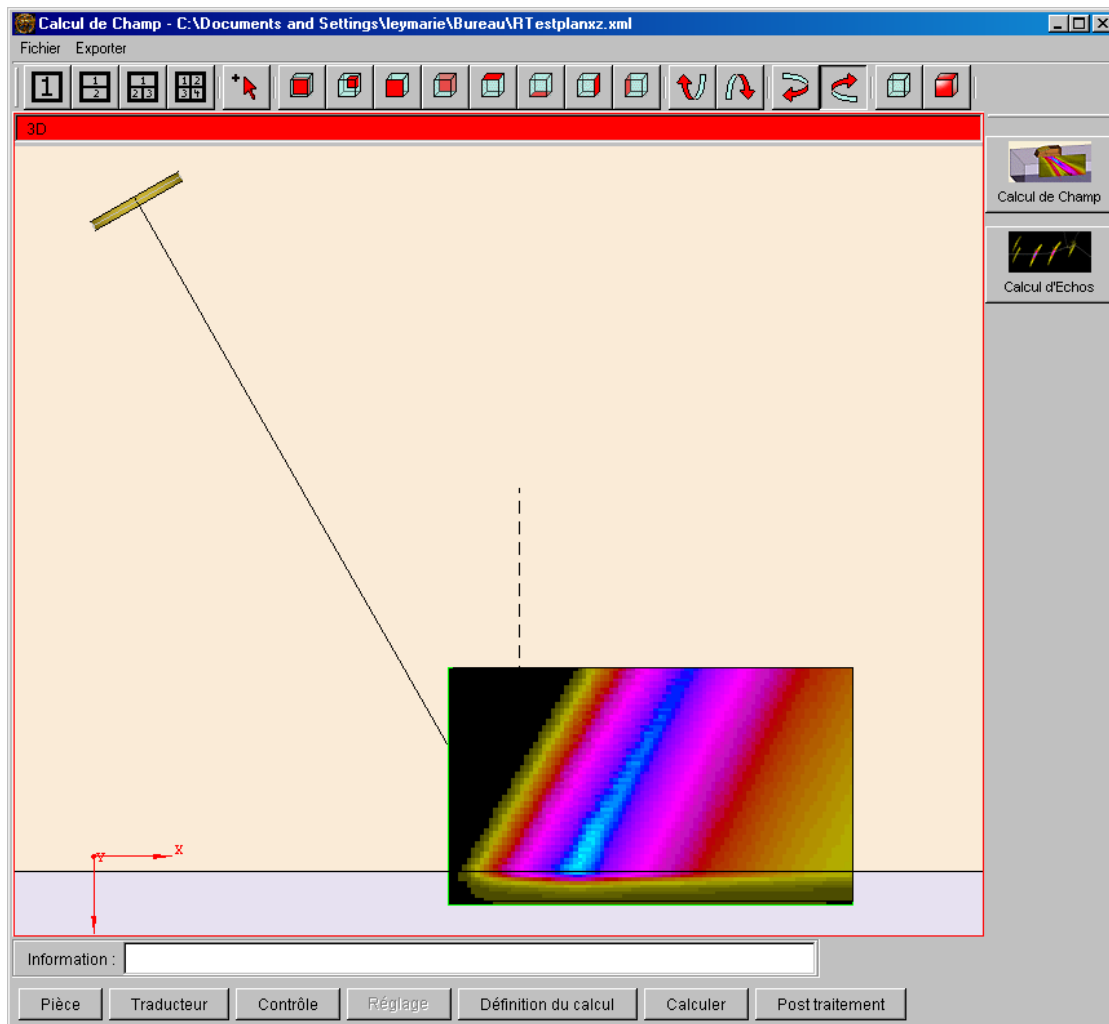


Figure 6: Prediction of field contribution of Rayleigh wave in the solid and leaky Rayleigh wave in the coupling fluid. Bulk wave contributions are not shown.

When computing together the bulk and surface wave components, typical interferences between bulk specular reflected beam and non-specular reflected contribution due to the leaky Rayleigh wave are observed leading to well-studied beam-shift or lateral beam displacement [9].

A more detailed view on these results is shown on Fig. 7 where results are displayed for field points along a vertical line. The curves are the maximum amplitude value one gets for the vertical component of the displacement, respectively. Typical amplitude variations of this component with depth are observed.

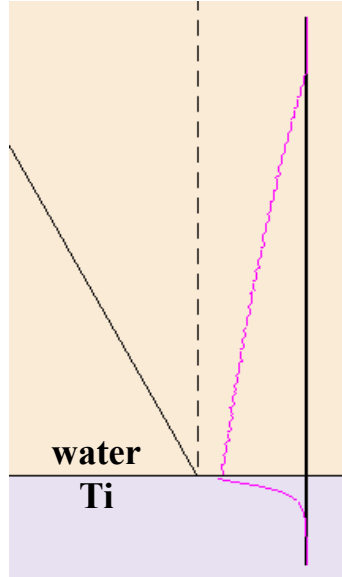


Figure 7: Prediction of vertical particle displacement associated to Rayleigh or leaky Rayleigh contributions for field points along a vertical line either in the fluid or in the solid.

Note again that results given in Figs. 6 and 7 account for transducer transient diffraction effects.

Discussion: In a configuration involving a non-planar interface, none of the integral formulations of the type of Eq. (2) is conceivable and therefore, no further asymptotic developments can be made. In the past, the same remark had been made in the development of a model for bulk waves transmitted through an arbitrary interface; in that case, the geometrical interpretation in terms of pencils was developed as the solution to get over this basic difficulty [5]. Following the same approach for simulating configurations of inspection based on surface waves, a theoretical approach relying on the geometrical interpretation of the terms predicted by the asymptotic developments has been derived aiming at the development of generic objects.

Following the work of Keller and Karal [10], the geometrical interpretation given for a planar interface can be generalized to curved interfaces if the velocity of the surface wave traveling at the interface is known. The main difficulty is now to determine ray trajectories for a complex interface geometry and this is all the more difficult since Rayleigh wavespeed depends on local curvatures of the surface and on frequency [11,12]. However, as the following table shows, dispersion of Rayleigh wavespeed is negligible when curvatures are large compared to the wavelength. For a titanium specimen, the Rayleigh wave dispersion is below 1% for curvature radius to wavelength ratios of 30 (Table 2). There are many applications involving UT with Rayleigh waves in which the approximation consisting in considering that there is no dispersion is valid.

R_n/λ	R_t/λ	c_R variation
10	10	2.9 %
30	30	1.0 %
50	100	0.6 %
100	∞	0.3 %

Table 2: Rayleigh wave velocity variation for different curvature radius to wavelength ratios. R_n is the radius in the propagation plane along the curvature; R_t is the radius normal to the propagation plane.

Once the wavespeed is known, ray paths can be determined using classical algorithms of differential geometry [13]. For simple interface geometries such as spherical and cylindrical interfaces, ray paths are even known analytically.

Conclusions: A new model for simulating ultrasonic inspections using surface waves has been developed. The kernel of the computation concerned with the prediction of surface wave generation, propagation and possible leakage is based on asymptotic developments of an exact integral formulation. Asymptotic developments have been

validated by comparison with exact results. The proposed development is easily interpreted geometrically so that a pencil theory for the configuration of interest has been derived. This latter theory is straightforwardly compatible with the existing pencil method previously developed for bulk elastic waves. Therefore, CIVA modeling tools can now deal with bulk waves together with surface wave generation.

As far as beam / defect interaction is concerned, existing scattering theory implemented in CIVA can also be used straightforwardly since the incident field in the absence of a defect is an input of the simulation tool, whatever the nature of this field.

The pencil approach will help further developments of this simulation tool to deal with parts made of heterogeneous media. It is also believed that asymptotic solutions for head waves could be derived and interpreted as pencils for further inclusion in CIVA. Head waves are not a primary interest for NDT applications but can lead to supplementary contributions that may be misinterpreted if not accounted for in the simulation.

References:

- [1] J. Amos, J. Gray, A. Lhémery and R. B. Thompson, "Future applications of NDE simulators", *Review of Progress in QNDE* **23**, ed. by D. O. Thompson and D. E. Chimenti (AIP Conference Proceedings 700, Melville, 2004), pp. 1620-1632.
- [2] Informations about CIVA can be found on the website <http://www-civa.cea.fr>
- [3] D. Frénet, P. Calmon and M. Ouafouh, "Generation of leaky Rayleigh waves using a conical phased-array transducer: Modeling time domain signals reflected on anisotropic materials", in proceedings of the 98' *IEEE Ultrasonics Symposium*, ed. by S. C. Schneider, M. Levy and B. R. McAvoy, (IEEE, N.-Y, 1998), pp. 269-272.
- [4] L. Butin and A. Lhémery, "A transient model for the simulation of ultrasonic nondestructive experiments including surface wave effects on cracks", *Review of Progress in QNDE* **18**, ed. by D. O. Thompson and D. E. Chimenti (Kluwer Academic/Plenum, N.-Y., 1999), pp. 135-142.
- [5] N. Gengembre and A. Lhémery, "Pencil method in elastodynamics. Application to ultrasonic field computation", *Ultrasonics* **38** (2000), pp. 495-499.
- [6] H. Lamb, "On the propagation of tremors over the surface of an elastic solid", *Phil. Trans. Royal Soc. London* **203** (1904), pp.1-42.
- [7] L. M. Brekhovskikh, *Waves in layered media* (Academic Press, New York, 1980).
- [8] H. Überall, Surface waves in acoustics, in *Physical Acoustics: Principles and Methods* (Academic, New York, 1973), Vol. 10, Chap. 1.
- [9] H. L. Bertoni and T. Tamir, "Unified theory of Rayleigh-angle phenomena for acoustic beams at liquid-solid interfaces", *Appl. Phys.* **2** (1973), pp. 157-172.
- [10] J. B. Keller and C. Karal Jr., "Surface wave excitation and Propagation", *J. Appl. Phys.* **31** (1960), pp. 1039-1046.
- [11] I. A. Viktorov, *Rayleigh and Lamb waves*, (Plenum Press, New York, 1967).
- [12] V. G. Mozhaev, "Application of the perturbation method for calculating the characteristics of surface waves in anisotropic and isotropic solids with curved boundaries", *Sov. Phys. Acoust.* **30** (1984), pp. 397-400. [13] R. L. Barger, "Trajectory fitting in function space with application to analytic modelling of surfaces", NASA Technical Paper 3232 (1992).

